Infrared Spectra of Magnesium Hydride Molecules, Complexes, and Solid Magnesium Dihydride

Xuefeng Wang and Lester Andrews*

Department of Chemistry, University of Virginia, Charlottesville, Virginia 22904-4319

Received: August 10, 2004; In Final Form: September 29, 2004

Laser-ablated Mg atoms react with molecular hydrogen to give magnesium hydrides during condensation in excess hydrogen and neon for characterization by matrix infrared spectroscopy. The observed absorptions are identified by isotopic substitution and theoretical calculations of vibrational fundamentals and assigned to the MgH, MgH_2, Mg_2H, Mg_2H_2, Mg_2H_3, and Mg_2H_4 molecules. Subsequent UV irradiation excites Mg to the ^1P state, which inserts into H_2 and markedly increases the yield of MgH_2 and Mg_2H_4. Interesting $MgH_2(H_2)_n$ complexes are formed with high yield in solid hydrogen. Mg_2H_4 is a dibridged molecule analogous to dialane. Sample annealing gives MgH_2 polymers, which favor single bridge-bond linkages. Warming above 8 K allows the H_2 matrix to evaporate and solid MgH_2 to form with broad 1160 and 560 cm^{-1} absorptions that remain on the window at 300 K. Thus, we have reacted the elements to give the stable MgH_2 molecule, formed its dimer and tetramer, and finally obtained the ultimate polymer, solid MgH_2, which is of interest for hydrogen storage.

Introduction

Magnesium hydrides continue to be of interest as promising materials for hydrogen storage.[1−3] MgH_2 is a stable molecule with a high hydrogen storage capacity (7.6 wt %). However, reversibility of the thermal absorption/desorption is very poor, and a temperature near 300 °C is required for 1 bar of hydrogen gas. Experiments show that magnesium hydride formation from bulk Mg and H_2 gas is very slow, but Mg alloys with transition metals react with molecular hydrogen to form hydrides fairly rapidly where transition metals act as a catalyst to decompose molecular hydrogen. Magnesium hydride solid forms the rutile structure, and vibrational spectra have been recorded by inelastic-neutron and Raman scattering.[4,5] The gaseous linear MgH_2 molecule has recently been observed in an electrical discharge through the vibration−rotation emission spectrum.[6]

The reaction of laser-ablated Mg atom with H_2 in excess argon has been studied in this group, and the magnesium hydride molecules MgH, Mg_2H_2, MgH_2, and Mg_2H_4 have been identified.[7] Magnesium dihydride has also been observed in solid krypton and xenon.[8] Recently we reported the preparation of dialane (Al_2H_6) using the reaction of laser-ablated aluminum with pure H_2 during codensation at 3.5 K.[9−11] The AlH generated from laser ablation further reacts with H_2 to give AlH_3 upon UV photolysis, which dimerizes to form Al_2H_6.[9,10] Evidence for trialane (Al_3H_9) and tetraalane (Al_4H_{12}) as stable molecules was found in our later investigation.[11] Similarly gallium, indium, and thallium hydride molecules have been prepared and investigated in solid hydrogen, and solid Ga and In hydrides were formed on evaporation of the hydrogen matrix.[12−15]

We present here a new matrix isolation study of laser-ablated magnesium atom reactions with H_2 in solid hydrogen and neon. The higher magnesium hydrides Mg_2H_2, Mg_2H_3, Mg_2H_4, Mg_3H_6, and Mg_4H_8 and hydrogen complexes $MgH_2(H_2)_n$ are identified by matrix infrared spectroscopy and density functional theoretical calculations. The characterization of higher magnesium hydrides and dihydrogen complexes can provide important molecular structure information for approaching more efficient Mg-based hydrogen-storage materials.

Experimental and Computational Methods

The experiments for reactions of laser-ablated magnesium atoms with hydrogen during condensation in excess hydrogen and neon have been described in detail previously.[16−18] The Nd:YAG laser fundamental (1064 nm, 10 Hz repetition rate with 10 ns pulse width) was focused onto a rotating normal magnesium target (Fisher) or ^{26}Mg plate (Oak Ridge National Laboratory). The laser energy was varied from 5 to 20 mJ/pulse. Laser ablated magnesium atoms were co-deposited with hydrogen (0.2 to 4%) in excess neon or pure hydrogen onto a 3.8 K CsI cryogenic window at 2−4 mmol/h (H_2/Ne for 1 h and pure H_2 for 30 min). Isotopic D_2 and HD (Cambridge Isotopic Laboratories) and selected mixtures were used in different experiments. FTIR spectra were recorded at 0.5 and 0.13 cm^{-1} resolution on a Nicolet 750 with 0.1 cm^{-1} accuracy, using an HgCdTe detector. Matrix samples were annealed at different temperatures, and selected samples were subjected to broadband photolysis by a medium-pressure mercury arc lamp (Philips, 175W) with the globe removed or ArF eximer (193 nm) irradiation (Optex). A simple and efficient converter was used to prepare parahydrogen and several spectra of Mg atom reaction with p-H_2 were collected.[19] Emission spectra were recorded with an Ocean Optics optical fiber spectrometer.[20]

The density functional theoretical calculations of magnesium hydrides and hydride hydrogen complexes are given for comparison. The Gaussian 98 program[21] was employed to calculate the structures and frequencies of expected molecules, using the B3LYP functional and the MP2 method. The 6-311++G(3df,3pd) basis set for both Mg and H atoms was used. All the geometrical parameters were fully optimized and

* Address correspondence to this author. E-mail: lsa@virginia.edu.

10.1021/jp046410h CCC: $27.50 © 2004 American Chemical Society
Published on Web 12/08/2004

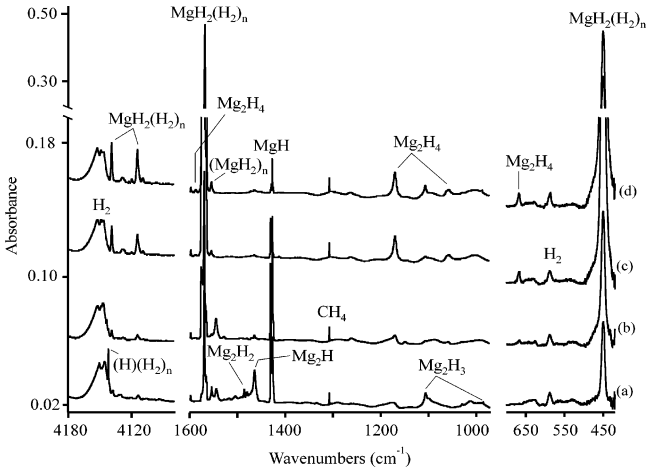

Figure 1. Infrared spectra in selected regions for laser-ablated Mg co-deposited with n-H_2 at 3.8 K: (a) after deposition for 20 min, (b) after $\lambda > 320$ nm irradiation for 20 min, (c) after 240−380 nm irradiation for 20 min, and (d) after annealing to 6.6 K.

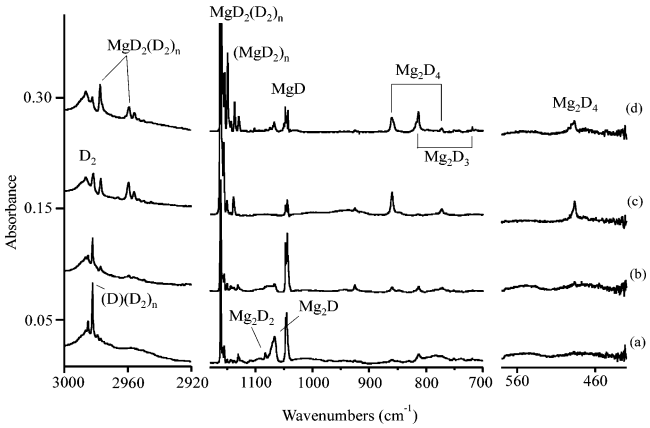

Figure 2. Infrared spectra in selected regions for laser-ablated Mg co-deposited with n-D_2 at 3.8 K: (a) after deposition for 20 min, (b) after $\lambda > 320$ nm irradiation for 20 min, (c) after $\lambda > 240$ nm irradiation for 20 min, and (d) after annealing to 10.5 K.

the harmonic vibrational frequencies were obtained analytically at the optimized structures.

Results

Experimental spectra are presented for magnesium atom reactions with H_2, D_2, HD, and the $H_2 + D_2$ mixture in excess neon and solid molecular hydrogen. Similar experiments have been done in parahydrogen and orthodeuterium for comparison.[22,23] Common absorptions, namely those assigned to $H(H_2)_n$ and $H^-(H_2)_n$, have been reported previously,[18,24] and are not discussed here. Trace impurity CO_2, CO, H_2O, and CH_4 appeared in all experiments but no impurity reaction products were observed with these molecules. New DFT and MP2 calculations of magnesium hydrides and hydrogen complexes are given for identification purposes.

Infrared Spectra. Figure 1 shows the spectra of laser-ablated magnesium atom with pure normal H_2 during co-deposition at 3.8 K, and the absorptions are listed in Table 1. After deposition new bands at 4139.0, 4114.5, 1569.5 (site splitting at 1576.4 cm^{-1}), and 450.1 cm^{-1} (group A), weak bands at 1587.6, 1170.5, 1058.7, and 667.2 cm^{-1} (group B), a strong 1427.1 cm^{-1} band (site splittings at 1429.5, 1430.6, and 1431.9 cm^{-1}), and weak absorptions at 1464.6 and 1105.9 cm^{-1} were observed. Irradiation at $\lambda > 320$ nm increased the group A and B bands, markedly reduced the 1464.6 and 1105.9 cm^{-1} absorptions, and decreased the 1544.3 cm^{-1} satellite. Subsequent 240−380 nm irradiation increased group A and B bands by a factor of 6, and the following $\lambda > 240$ nm irradiation increased group A and decreased group B. Annealing to 6.6 K then decreased the group A and increased the group B bands (Figure 1d). A subsequent annealing to 8.0 K (not shown) decreased the group A and B bands, sharpened the major band at 1569.2 cm^{-1}, revealed magnesium isotopic splittings at 1566.9 and 1565.2 cm^{-1}, and further increased a 1554.5 cm^{-1} satellite absorption. In solid normal deuterium group A bands shift to 2977.2, 2959.5, and 1161.4 cm^{-1} (the 450.1 cm^{-1} band shifts out of our measure-

TABLE 1: Infrared Absorptions (cm^{-1}) Observed from Reactions of Magnesium and Dihydrogen in Excess Hydrogen

Mg n-H_2	Mg p-H_2	^{26}Mg n-H_2	Mg n-D_2	Mg o-D_2	^{26}Mg n-D_2	HD	identification
4139.0	4148.8	4139.0	2977.2	2986.7	2977.2	3620.0	$MgH_2(H_2)_n$
4114.5	4128.0	4114.5	2959.5	2959.8	2959.5	3597.6	$MgH_2(H_2)_n$
3078.8	3091.6	3073.0	2249.4	2252.3	2242.7		$MgH_2(H_2)_n$ (overtone)
						1594.0, 1592.6	$Mg_2H_2D_2$
1587.6		1583.7					Mg_2H_4
1576.4			1163.2				$MgH_2(H_2)_n$ (site)
1569.5	1577.4[a]	1565.2	1161.4	1163.7	1155.9	1575.6, 1166.0	$MgH_2(H_2)_n$
1554.5			1150.7			1554.4, 1130.3	$(MgH_2)_n$
1544.3	1546.6		1138.3	1140.6			(Mg_xH)
						1567.2, 1139.1	$MgHD(HD)_n$
1486.1	1491.6	1484.1	1083.0	1084.7	1080.8	1495.7, 1088.9	Mg_2H_2
1480.4		1478.5				1489.1, 1084.5	Mg_2H_2 (site)
1464.6	1466.7	1462.6	1066.6	1068.7	1063.8	1464.3, 1067.8	Mg_2H
1431.9		1429.8	1047.5	1048.0	1045.0	1433.5, 1046.9	MgH (site)
1430.6		1428.5	1045.9	1046.4	1043.4	1431.9, 1045.5	MgH (site)
1429.5	1429.9	1427.4	1044.4	1044.9	1041.8	1430.6, 1044.3	MgH (site)
1427.1	1427.4	1425.3	1042.8	1043.0	1039.9	1428.1, 1042.6	MgH
1170.5	1168.2	1169.0	859.9	859.8	857.9	1169, 1146.3	Mg_2H_4
						811.0, 807.9	HMg(HD)MgD
						860.8, 771.1	$HMg(D_2)MgH$
						1204.9, 655.5	$DMg(H_2)MgD$
1105.9	1106.8	1105.6	813.1	813.4	811.6	1013.9, 834.3	Mg_2H_3
1058.7	1057.1	1057.0	772.3	772.4	770.8		Mg_2H_4
985.5	986.1	985.1	718.5	718.6	717.7		Mg_2H_3
667.2	665.3	666.1	486.5	486.1	485.0	586.3, 505.3	Mg_2H_4
450.1	450.4	449.0					$MgH_2(H_2)_n$

[a] For ^{24}Mg: ^{25}Mg at 1575.1 cm^{-1}, ^{26}Mg at 1573.0 cm^{-1}. [b] For ^{24}Mg: ^{25}Mg at 1160.7 cm^{-1}, ^{26}Mg at 1157.7 cm^{-1}.

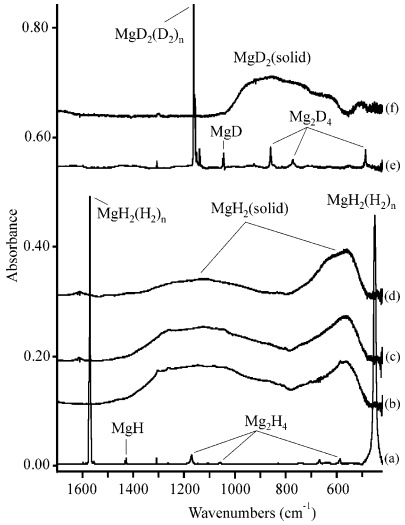

Figure 3. Infrared spectra in the 1700−420 cm^{-1} region for laser-ablated Mg co-deposited with hydrogen at 3.8 K: (a) after deposition with H_2 for 20 min and 240−380 nm irradiation for 20 min, (b) after warming to 10 K, (c) after warming to 200 K, (d) after warming to 300 K, (e) after co-deposition with D_2 for 20 min and $\lambda > 240$ nm irradiation for 20 min, and (f) after warming to 50 K.

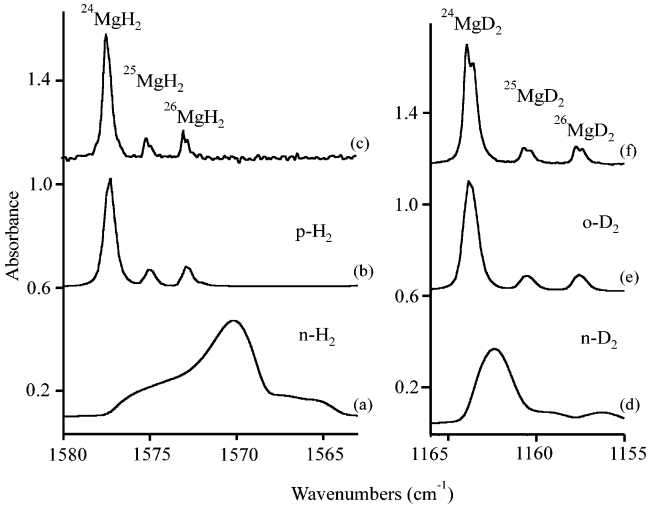

Figure 4. Infrared spectra of MgH_2 and MgD_2 in solid molecular hydrogens after $\lambda > 240$ nm irradiation at 3.8 K: (a) MgH_2 in n-H_2, (b) MgH_2 in *p*-H_2 (99%), (c) MgH_2 in *p*-H_2 (99%), 0.13 cm^{-1} resolution, (d) MgD_2 in n-D_2, (e) MgD_2 in *o*-D_2 (98%), and (f) MgD_2 in *o*-D_2 (98%), 0.13 cm^{-1} resolution.

ment region), and group B bands shift to 859.9, 772.3, and 486.5 cm^{-1} as shown in Figure 2. All other weak bands observed in solid hydrogen shift in solid deuterium as listed in Table 1. Analogous absorptions from ^{26}Mg atom reactions with H_2 in solid normal hydrogen and D_2 in solid normal deuterium gave small red-shifts as expected.

After warming above 8 K, the H_2 host evaporates and broad bands centered at 1160 and 560 cm^{-1} appear on the cold window. Spectra recorded at 10, 200, and 300 K (Figure 3b,c,d) reveal band broadening with increasing temperature. Spectra for an analogous deuterium sample give a broad counterpart centered at 880 cm^{-1} (Figure 3f).

The absorptions for reaction products of magnesium atom with H_2 in parahydrogen are also listed in the Table 1. The interaction in solid parahydrogen is reduced, the band contours are much sharper than in normal solid hydrogen,[25] and natural magnesium isotopic splittings are resolved. In addition the absorptions show slight blue-shifts in both p-H_2 and o-D_2. Figure

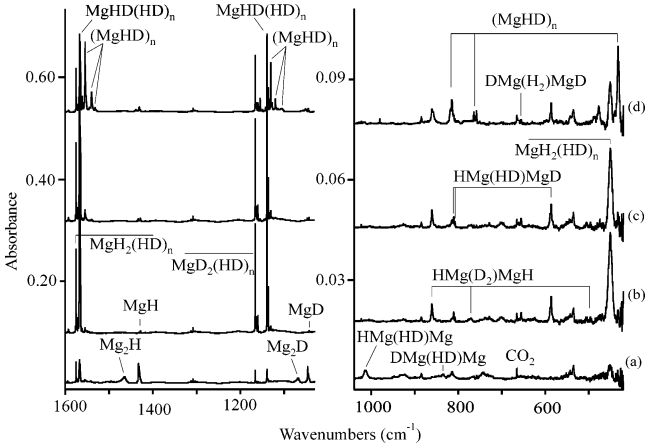

Figure 5. Infrared spectra in selected regions for laser-ablated Mg co-deposited with HD at 3.8 K: (a) after deposition for 20 min, (b) after 240−380 nm irradiation for 20 min, (c) after annealing to 8 K, and (d) after annealing to 9 K.

4 compares spectra in different nuclear spin isomers. Spectra recorded at 1/8 cm^{-1} resolution revealed site splittings about 0.3 cm^{-1} lower than the main magnesium isotopic peaks.

Infrared spectra for Mg in pure HD give sharp bands in both Mg-H and Mg-D stretching regions, as shown in Figure 5. An experiment was done with $H_2 + D_2$ (50−50) and the strong 1570.3 and 1162.2 cm^{-1} bands after 240−380 nm irradiation were 0.28 and 0.089 absorbance units, respectively, and weaker 1431.6 and 1045.9 cm^{-1} bands were 0.024 and 0.011 absorbance units.

The neon matrix spectra of reaction products of magnesium and molecular hydrogen are shown in Figure 6, and absorptions are listed in Table 2. The major absorptions at 1431.3 cm^{-1} and at 1574.0 and 450.4 cm^{-1} (group A) appeared on the Mg atom reaction with H_2 in excess neon during deposition. On $\lambda > 240$ nm photolysis group B bands were generated while group A bands increased markedly. On annealing to 9.5 K new bands at 1564.5 and 1551.6 cm^{-1} appeared and increased on further annealing. New absorptions with deuterium and deuterium hydride reagents are listed in Table 2.

Calculations. The linear structure of MgH_2 has been calculated with different theoretical methods.[7,26−28] By using B3LYP and MP2 the Mg−H bond length is predicted to be 1.701 and 1.704 Å, respectively, which are in very good agreement with the recent gas-phase value of 1.7033 Å.[6] The linear MgH_2 molecule is polarized to be $H^{\delta-}-Mg^{\delta+}-H^{\delta-}$, and as a result molecular hydrogen can be associated to $H^{\delta-}$ and $Mg^{\delta+}$ to form a large cluster. The coplanar $MgH_2(H_2)_4$ model complex is predicted to be stable local minimum with two H_2 are attached to the end $H^{\delta-}$ and the other two H_2 to $Mg^{\delta+}$. Apparently the interactions are slightly different, namely $H^{\delta-}\cdots HH$ is 2.740 Å while $Mg^{\delta+}\cdots H_2$ is 2.867 Å. The D_{4h} $MgH_2(H_2)_6$ model complex forms an even more stable local minimum, and the ligand distances decrease to 2.731 and 2.825 Å. Solid hydrogen is a perfect medium to study this cluster in which MgH_2 is trapped and infrared modes of H_2 attached to MgH_2 are activated. Tables 3 and 4 give the results of our calculations.

$Mg(H_2)^+$ and MgH_2^+ are calculated and $Mg(H_2)^+$ lies 46.6 kcal/mol lower at the B3LYP level. The strong H−H stretching mode should be detected if Mg^+ generated from laser ablation is trapped in solid hydrogen. Similar cations $M(H_2)^+$ have been calculated and observed for group 3A metals.[10−14] The MgH_2^- anion is bent and the electron affinity for MgH_2 is predicted to be only 4.7 kcal/mol.

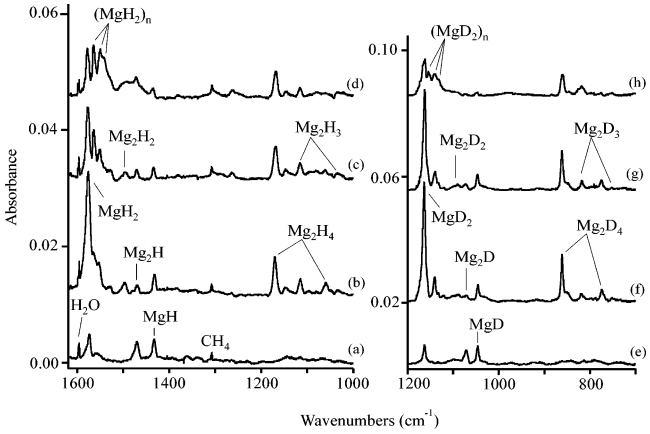

Figure 6. Infrared spectra for laser-ablated Mg in the 1620−1000 cm^{-1} region with Ne/H_2 and in the 1200−700 cm^{-1} region with Ne/D_2: (a) after deposition with 4% H_2 in neon for 60 min, (b) after $\lambda > 240$ nm irradiation for 20 min, (c) after annealing to 9 K, and (d) after annealing to 12 K, (e) after deposition with 4% D_2 in neon for 60 min, (f) after $\lambda > 240$ nm irradiation for 20 min, (g) after annealing to 9 K, and (h) after annealing to 13 K.

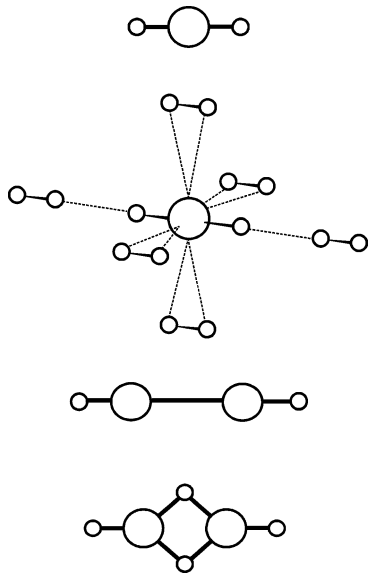

Figure 7. Calculated structures for MgH_2, $MgH_2(H_2)_6$, Mg_2H_2, and Mg_2H_4. Bond lengths and angles given in Table 3.

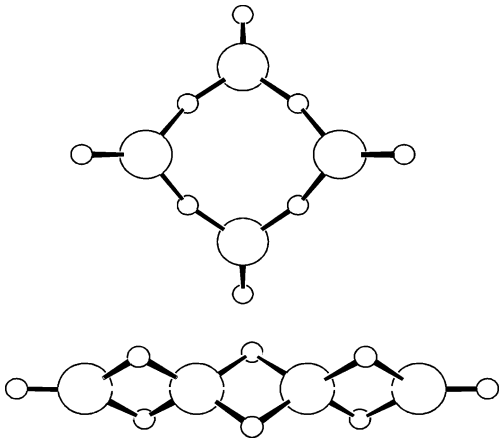

Figure 8. Calculated structures for cyclic and chain Mg_4H_8 isomers. Bond lengths and angles given in Table 3.

The dimer of MgH_2, $HMg(\mu\text{-}H)_2MgH$, has been theoretically investigated[29] and the doubly bridged planar D_{2h} structure has the lowest energy. Our B3LYP and MP2 calculations reach the same conclusions. Higher polymers Mg_3H_6 and Mg_4H_8 were calculated at the B3LYP level and slightly higher energy single-bridged (s-Mg_3H_6 and s-Mg_4H_8) and lower energy double-bridged (d-Mg_3H_6 and d-Mg_4H_8) hydrogen bonds were obtained. The double-bridged hydrogen bond lengths and bond angles are basically very close to Mg_2H_4, suggesting strong Mg−H−Mg stretching modes should be observed if such molecules are trapped in the matrix. However the single-bridged hydrogen bond lengths are shorter and angles are much larger, and the strongest IR absorptions are located in the Mg−H stretching region. Figures 7 and 8 compare several calculated structures.

Analogous calculations were done for MgH, Mg_2H radical, Mg_2H_2, and Mg_2H_3 radical. For the ground-state MgH 1.742 Å bond lengths and a 1461.6 cm^{-1} Mg−H stretching frequency are computed, which are very close to recent gas-phase experimental values of 1.7298 Å and 1431.98 cm^{-1}, respectively.[30] MP2 calculations give similar results. Two Mg_2H radical structures are located: MgMgH is lower than MgHMg by 2.6 kcal/mol. Two isomers of MgH dimer are found, and linear HMgMgH lies 10.5 kcal/mol lower in energy than rhombic $Mg(\mu\text{-}H)_2Mg$. For the Mg_2H_3 radical, single-bridged (s-Mg_2H_3) and double-bridged (d-Mg_2H_3) isomers are located on the potential energy surface. The d-Mg_2H_3 is 13.3 kcal/mol lower in energy and characterized by the strongest Mg−H−Mg stretching mode, but s-Mg_2H_3 with higher energy shows the strongest Mg−H stretching mode.

TABLE 2: Infrared Absorptions (cm^{-1}) Observed from Reactions of Magnesium and Dihydrogen in Excess Neon

H_2/Ne	D_2/Ne	HD/Ne	identification
1583.7			Mg_2H_4
1576.8	1163.2	1569.3, 1140.7	MgH_2 (phot)
1574.0	1162.4	1569.3, 1140.7	MgH_2 (dep)
1564.5	1140.6	1558.2, 1132.7	Mg_3H_6
1551.6	1140.6	1544.9, 1123.6	Mg_4H_8
1496.4	1088.9	1508.9, 1099.3	Mg_2H_2
1470.0	1070.9	1470.0, 1070.9	Mg_2H
1431.3	1046.2	1431.3, 1046.2	MgH
1169.9	860.8	1167.7, 862.1	Mg_2H_4
1114.6	818.5		Mg_2H_3
1058.9	773.6	761.5	Mg_2H_4
665.9	486.3		Mg_2H_4
450.4			MgH_2

Discussion

Infrared spectra of magnesium hydrides and dihydrogen complexes will be assigned on the basis of isotopic shifts and agreement with density functional calculations.

MgH_2. In solid neon the 1574.0 cm^{-1} band increased markedly on 240 nm photolysis and shifted to 1576.8 cm^{-1} (Figure 6), which tracks the 450.4 cm^{-1} absorption. These two bands can be assigned to Mg−H stretching and H−Mg−H bending modes of MgH_2 for the following reasons. The deuterium counterpart for the 1576.8 cm^{-1} band was found at 1163.2 cm^{-1}, giving a 1.3556 H/D isotopic frequency ratio, which is appropriate for the Mg−H stretching mode, but 450.4 cm^{-1} shifts out of our measurement region. With HD in neon two new strong bands at 1569.3 cm^{-1} in the Mg−H stretching region and at 1140.7 cm^{-1} in the Mg−D stretching region (H/D = 1.3756) were observed on 240 nm photolysis. The relationship of the HD product absorptions and the MgH_2 and MgD_2 bands demonstrates that two equivalent H(D) atoms are involved in the vibration and that an unobserved stretching mode appears at lower frequency. In solid argon the MgH_2 absorptions were observed at 1571.9 and 439.8 cm^{-1}.[7] The antisymmetric

TABLE 3: Magnesium Hydride Geometries, Vibrational Frequencies (cm^{-1}), and Intensities Calculated at the B3LYP/6-311++G(3df,3pd) Level of Theory

species	structure[a]	E[b]	frequencies, cm^{-1} (intensities, km/mol)
MgH ($^2\Sigma$)	MgH: 1.742	0.0	MgH: 1461.6 (252) MgD: 1054.5 (131)
MgH^- ($^1\Sigma$)	MgH: 1.877		MgH^-: 1088.4 (2325) MgD^-: 785.3 (1151)
MgH_2 ($^1\Sigma_g^+$)	MgH: 1.701 HMgH: 180.0	0.0	MgH_2: 1637.3 (σ_u, 440), 1613.2 (σ_g, 0), 428.3 (π_u, 472 × 2) MgD_2: 1202.2 (237), 1141.2 (0), 314.5 (245 × 2)
MgH_2^- ($^2A_1$)	MgH: 1.782 HMgH: 125.4	−4.7	MgH_2^-: 1342.3 (b_2, 689), 1327.7 (a_1, 1240), 529.3 (a_1, 1295)
$Mg(H_2)^+$ ($^2A_1$)	MgH: 2.573 HH: 0.751	171.9	$Mg(H_2)^+$: 4289.6 (a_1, 160), 371.9 (b_2, 17), 265.1 (a_1, 73)
MgH_2^+ ($^2\Sigma_u^+$)	MgH: 1.788	218.5	MgH_2^+: 1312.2 (σ_g, 0), 1016.5 (σ_u, 2036), 121.2 (π_u, 71 × 2)
MgH_3^- ($^1A_1'$)	MgH: 1.804 HMgH: 120.0		MgH_3^-: 1356.3 (0), 1275.2 (e′, 945 × 2), 608.6 (e′, 495 × 2), 552.7 (a_2'', 776)
$MgH_2(H_2)_4$ (D_{2h})	MgH: 1.702 MgH′: 2.857 H′H′: 0.745 HH″: 2.740 H″H″: 0.744		$MgH_2(H_2)_4$: 4390.4 (a_g, 0), 4390.3 (b_{1u}, 26), 4368.6 (a_g, 0), 4368.1 (b_{2u}, 5), 1631.6 (b_{1u}, 515), 453.6 (b_{2u}, 541), 436.5 (b_{3u}, 433), ...
$MgH_2(H_2)_6$ (D_{4h})	MgH: 1.703 MgH′: 2.825 H′H′: 0.746 HH″: 2.713 H″H″: 0.744		$MgH_2(H_2)_6$: 4387.8 (a_{1g}, 0), 4387.6 (a_{2u}, 31), 4366.8 (a_{1g}, 0), 4366.3 (b_{3g}, 0), 4365.9 (e_u, 4 × 2), 1623.7 (a_{2u}, 520), 1605.2 (0), 459.2 (e_{2u}, 519 × 2), ... $MgD_2(D_2)_6$: 3103.9 (0), 3103.7 (15), 3089.0 (0), 3088.6 (0), 3088.4 (2 × 2), 1192.0 (275), 1135.5 (0), 332.8 (285 × 2), ...
MgMgH ($^2\Sigma$)	MgMg′: 3.072 MgH: 1.734	0.0	MgMgH: 1506.7 (σ, 718), 185.0 (σ, 1), 128.3 (σ, 92 × 2) MgMgD: 1087.5 (371), 183.2 (1), 96.7 (48 × 2)
MgHMg ($^2\Sigma^+$)	MgH: 1.951	2.6	MgHMg: 863.9 (σ_u, 1596), 309.1 (π_u, 7 × 2), 208.1 (σ_g, 0)
Mg_2H_2 ($^1\Sigma_g^+$) (linear)	MgH: 1.721 MgMg: 2.867	0.0	Mg_2H_2: 1572.0 (σ_g, 0), 1551.3 (σ_u, 1082), 300.5 (π_g, 0 × 2), 269.1 (σ_g, 0), 244.6 (π_u, 246 × 2) Mg_2D_2: 1135.1 (0), 1119.2 (563), 263.6 (0), 230.0 (0 × 2), 176.5 (128 × 2) HMg_2D: 1561.8 (525), 1127.0 (298), ...
Mg_2H_2 (^1A_g) (rhomb)	MgH: 1.915 MgHMg: 95.9	10.5	Mg_2H_2: 1278.6 (a_g, 0), 1029.9 (b_{2u}, 349), 982.6 (b_{3g}, 0), 700.0 (b_{1u}, 675), 631.8 (b_{3u}, 134), 316.7 (a_g, 0)
d-Mg_2H_3 ($^2A_1$) (DB)	MgH: 1.872 Mg′H: 1.905 MgH′: 1.700	0.0	Mg_2H_3: 1615.2 (288), 1292.5 (81), 1162.2 (1047), 1042.8 (451), 1025.9 (70), 596.0 (162), 336.3 (117), 322.5 (3), 229.4 (153) Mg_2D_3: 1165.9 (182), 917.7 (52), 836.4 (515), 753.8 (239), 732.2 (36), 434.8 (93), 318.5 (3), 250.8 (61), 169.0 (78)
s-Mg_2H_3 ($^2A_1$) (SB)	MgH: 1.878 MgH′: 1.698	13.3	Mg_2H_3: 1623.1 (1), 1610.5 (659), 1140.1 (245), 1060.6 (481), 348.2 (265), 275.5 (0), 251.5 (18), 222.4 (23), 215.8 (253)
Mg_2H_4 (^1A_g) (D_{2h})	MgH: 1.875 MgH′: 1.694 MgHMg: 95.6		Mg_2H_4: 1640.7 (a_g, 0), 1632.7 (b_{1u}, 418), 1308.1 (a_g, 0), 1238.9 (b_{1u}, 1135), 1104.6 (b_{3g}, 0), 1083.6 (b_{2u}, 630), 671.7 (b_{3u}, 488), 373.1 (b_{2u}, 347), 330.0 (a_g, 0), 311.8 (b_{3g}, 0), 298.7 (b_{2g}, 0), 218.8 (b_{3u}, 262) Mg_2D_4: 1185.6 (0), 1176.9 (283), 927.3 (0), 892.7 (551), 786.1 (0), 784.5 (351), 489.5 (272), 322.3 (0), 267.7 (176), 239.7 (0), 228.8 (0), 155.9 (132)
s-Mg_3H_6	MgH: 1.697 MgH′: 1.828 MgH′Mg: 139.1	0.0	Mg_3H_6: 1646.1 (e′, 85 × 2), 1633.1 (a_1', 0), 1599.9 (e′, 1404 × 2), 1505.9 (a_2', 0), 935.8 (a_1', 0), 798.6 (e′, 619 × 2), 629.8 (a_2'', 795), 406.7 (e″, 0 × 2), ..., 147.7 (e″, 0 × 2)
d-Mg_3H_6	MgH: 1.693 MgH′: 1.862 MgH′Mg: 94.0	−3.8	Mg_3H_6: 1638.5 (a_1, 0), 1636.1 (b_2, 402), ..., 1204.5 (b_2, 2504), 1078.2 (e, 456 × 2), 654.9 (e, 290 × 2), ..., 68.2 (e, 13 × 2)
s-Mg_4H_8	MgH: 1.698 MgH′: 1.814 MgH′Mg: 163.3	0.0	Mg_4H_8: 1769.4 (b_2, 116), 1730.8 (e, 1208 × 2), 1632.8 (a_1, 0), 1618.1 (e, 878 × 2), 1616.7 (b_2, 199), 1615.3 (a_2, 0), 756.6 (a_1, 0), 642.4 (e, 979 × 2), 618.1 (b_2, 998), ..., 21.5 (a_1, 0)
d-Mg_4H_8	MgH: 1.694 MgH′: 1.866 MgH′Mg: 94.0	−12.7	Mg_4H_8: 1637.6 (a_g, 0), 1636.5 (b_{3u}, 402), 1178.5 (b_{3u}, 4054), 1117.8 (b_{2u}, 361), ..., 1095.4 (b_{1u}, 639), 1088.3 (b_{2u}, 852), ..., 38.6 (b_{2u}, 5)

[a] Bond lengths (Å), angles (deg). [b] Relative energies of stoichiometric species (kcal/mol).

stretching mode of MgH_2 was measured in the gas phase at 1586.7 cm^{-1} and MgD_2 at 1176.5 cm^{-1}, which gives a slightly lower H/D frequency ratio.[6] The gas and argon measurements bracket our neon matrix value.

Calculation with B3LYP/6-311++G(3df,3pd) gave MgH_2 with a linear structure and a strong Mg−H antisymmetric stretching mode at 1637.3 cm^{-1} (σ_u) and a bending mode at 428.3 cm^{-1} (π_u), which reproduce experimental observations. We expect that the bending mode will appear around 460 cm^{-1} in the gas-phase molecule.

$MgH_2(H_2)_n$. In solid, normal hydrogen bands at 1569.5 cm^{-1} (site splitting at 1576.4 cm^{-1}) (Mg−H stretching) and 450.1 cm^{-1} (H−Mg−H bending) appeared on deposition and increased by 6-fold on 240−380 nm photolysis. A sharp band at 3078.8 cm^{-1} tracks the 1569.5 cm^{-1} band and must be the overtone of the Mg−H stretching mode. The 3078.8 cm^{-1} band is 60.2 cm^{-1} less than 1569.5 × 2 = 3139.0 cm^{-1}, which is appropriate for anharmonicity. In solid parahydrogen, analogous strong bands observed at 1577.4 and 450.4 cm^{-1}, and an overtone at 3091.6 cm^{-1} show slight blue-shifts. The deuterium counterpart was found at 1161.4 cm^{-1} (site splitting at 1163.2 cm^{-1}) in pure normal D_2 and at 1163.7 cm^{-1} in ortho D_2. In pure HD two strong bands at 1567.2 and 1139.1 cm^{-1} were observed. Comparing neon spectra, these bands are appropriate for MgH_2, MgD_2, and MgHD. However, in pure H_2 two bands at 4139.0 and 4114.5 cm^{-1} near the H_2 fundamental track the

TABLE 4: Calculated Geometries, Vibrational Frequencies (cm^{-1}), and Intensities at the MP2/6-311++G(3df,3pd) Level

species	structure (Å, deg)	frequencies, cm^{-1} (intensities, km/mol)
MgH ($^2\Sigma$)	MgH: 1.729	MgH: 1556.2 (368) MgD: 1122.8 (191)
MgH_2 ($^1\Sigma_g^+$)	MgH: 1.704 HMgH: 180.0	MgH_2: 1659.4 (σ_u, 465), 1639.1 (σ_g, 0), 441.5 (π_u, 568 × 2) MgD_2: 1218.4 (251), 1159.5 (0), 324.1 (306 × 2)
$MgH_2(H_2)_4$ ($^1A_1$)	MgH: 1.705 HMgH: 180 MgH′: 2.780 H′H′: 0.740 HH″: 2.687 H″H″: 0.738	$MgH_2(H_2)_4$: 4494.7 (0), 4494.5 (22), 4463.9 (0), 4463.4 (9), 1655.3 (534), 1637.5 (0), 474.4 (615), 442.4 (522), ...
MgMgH ($^2\Sigma$)	MgMg′: 3.072 MgH: 1.734	MgMgH: 1651.5 (σ, 317), 383.2 (π, 4 × 2), 319.7 (σ, 50), 296.6 (π, 115 × 2) MgMgD: 1119.0 (185), 286.3 (1 × 2), 316.5 (53), 221.6 (54 × 2)
Mg_2H_2 ($^1\Sigma_g^+$)	MgH: 1.721 MgMg: 2.893	Mg_2H_2: 1601.9 (σ_g, 0), 1581.4 (σ_u, 1078), 312.3 (π_g, 0 × 2), 275.6 (σ_g, 0), 258.6 (π_u,290 × 2) Mg_2D_2: 1156.6 (0), 1141.0 (561), 269.9 (0), 238.7 (0 × 2), 186.6 (151 × 2)
d-Mg_2H_3 ($^2A_1$)	MgH: 1.704 MgH′: 1.872 Mg′H′: 1.904 MgMg′: 2.828	Mg_2H_3: 1641.0 (a_1, 279), 1321.9 (a_1, 190), 1218.9 (a_1, 1230), 1070.3 (b_2, 57), 1054.6 (b_2, 517), 606.5 (b_1, 154), 344.6 (b_2, 142), 329.7 (a_1, 3), 244.5 (b_1, 195)
Mg_2H_4 (^1A_g)	MgH: 1.877 MgH′: 1.699 MgHMg: 96.1	Mg_2H_4: 1660.9 (a_g, 0), 1652.3 (446), 1331.9 (a_g, 0), 1281.0 (b_{1u}, 1220), 1141.4 (b_{3g}, 0), 1097.1 (b_{2u}, 701), 687.1 (b_{3u}, 579), 377.2 (b_{2u}, 414), 335.0 (a_g, 0), 320.2 (b_{3g}, 0), 301.6 (b_{2g}, 0), 225.1 (b_{3u}, 312) Mg_2D_4: 1200.1 (0), 1190.8 (308), 944.2 (0), 923.2 (588), 812.7 (0), 794.3 (391), 500.7 (322), ...

1569.5 cm^{-1} band, and these bands are due to H−H stretching vibrations perturbed by HMgH. In solid D_2 analogous bands were observed at 2977.2 and 2959.5 cm^{-1} and in solid HD at 3620.0 and 3597.6 cm^{-1}. Clearly MgH_2 is coordinated by surrounding H_2 molecules in solid hydrogen. In addition ^{26}Mg reaction with H_2 gave slightly red-shifted bands at 1565.2 and 449.0 cm^{-1} and the overtone at 3073.0 cm^{-1}. Finally, the sharp natural Mg-isotopic splittings observed on annealing to 8.0 K show that a single Mg atom is involved in this product species.

The H/D isotopic frequency ratios for MgH_2/MgD_2 in the normal solids (1.3493) and the $J = 0$ solids (1.3555) are slightly different, but the latter matches the ratio in solid neon and the former is almost the same as the gas-phase isotopic frequency ratio.

Identification of the MgH_2 complex is further supported by quantum chemical calculations. As H_2 molecules are added to MgH_2, two different interactions are obtained, namely side-on H_2 to Mg and end-on H_2 to H. A $MgH_2(H_2)_6$ model complex calculated with the B3LYP functional, Figure 7, is a local minimum with end-on H_2 bonds slightly stronger than side-on H_2. As a result two different H−H stretching modes at 4387.6 and 4365.9 cm^{-1} are obtained. The two H−H stretching modes are predicated 19.7 and 41.5 cm^{-1} lower than that of free H_2, which are basically what is observed in solid hydrogen. In normal hydrogen two new H−H stretching frequencies at 4139.0 and 4114.5 cm^{-1} are 13.8 and 38.3 cm^{-1} below the solid H_2 fundamental (4152.8 cm^{-1}). MP2 calculations gave analogous results for $MgH_2(H_2)_4$, but the frequency calculation failed to converge for $MgH_2(H_2)_6$. Of course for MgH_2 trapped in a solid H_2 lattice even more H_2 molecules surround and stabilize the first shell $MgH_2(H_2)_6$ complex. Unfortunately, this complex decomposes when the hydrogen matrix evaporates and solid MgH_2 forms.

The insertion reaction of Mg into H_2 is endothermic by 4.1 kcal/mol from B3LYP and 2.9 kcal/mol from MP2 calculations. The insertion of ground-state Mg (3s,^{1}S) into H_2 is greatly inhibited by a large energy barrier, but the yield of MgH_2 increases greatly on 240 nm photolysis, so the Mg atom must be excited to the electronic state (3s3p, ^{1}P) by 240 nm to surmount the energy barrier and insert into H_2. In fact MgH_2 was observed on deposition since on laser ablation strong Mg ($^1P \rightarrow {}^1S$) emission at 284 nm was recorded in this experiment, and MgH_2 is generated and trapped in the matrix.

$$Mg^* + H_2 \rightarrow MgH_2\,(^1\Sigma_g^+) \quad (1)$$

$$MgH_2\,(^1\Sigma_g^+) + nH_2 \rightarrow MgH_2(H_2)_n \quad (2)$$

Mg_2H_4. The bands at 1587.6, 1170.5, 1058.7, and 667.2 cm^{-1} track together in solid normal hydrogen and blue shift several wavenumbers in solid parahydrogen (Table 1). As shown in Figure 1 these bands were barely observed after deposition (trace a) but increased on $\lambda > 320$ nm photolysis and increased greatly on 240−380 nm irradiation. However, $\lambda > 240$ nm broad-band photolysis reduced these bands by 30%, but 240−380 nm irradiation restored them totally. Since MgH_2 increased markedly and dimerization of MgH_2 is feasible under these conditions, we can assign these bands to Mg_2H_4. The 1587.6 cm^{-1} band is slightly higher than the Mg−H stretching mode of MgH_2, which is appropriate for the terminal Mg−H stretching mode in Mg_2H_4. The 1170.5 and 1058.7 cm^{-1} bands are located in the bridge bond stretching region and Mg(μ-H)$_2$Mg bridge-bond stretching modes are suggested. Recall the vibrations of the Al(μ-H)$_2$Al moiety in dialane Al_2H_6:[9,10] The 1170.5 and 1058.7 cm^{-1} bands are due to antisymmetric stretching modes parallel and perpendicular, respectively, to the Mg−Mg axis. The 667.2 cm^{-1} band arises from bending of bridge and terminal hydrogen atoms.

In solid normal deuterium 859.9, 772.3, and 486.5 cm^{-1} bands show the same photochemical behavior and must be assigned to Mg_2D_4. Similar experiments were done with orthodeuterium and these bands exhibit several wavenumber blue shifts. It is easy to assign the 859.9 and 772.3 cm^{-1} bands to Mg(μ-D)$_2$-Mg motion and the 486.5 cm^{-1} band as a bending mode in this molecule. Unfortunately the terminal Mg−D stretching mode for Mg_2D_4 is not observed since larger isotopic shift for this mode red-shifts it under the Mg−D stretching vibration of MgD_2.

The assignment of Mg_2H_4 is nicely supported by theoretical calculations. The most stable structure for the dimer of MgH_2 is the dihydrogen bridge linkage H−Mg(μ-H)$_2$Mg−H. The four strongest IR active modes calculated at the B3LYP/6-311++G-(3df,3pd) level of theory are 1632.7 (b_{1u}), 1238.9 (b_{1u}), 1083.6 (b_{2u}), and 671.7 (b_{3u}) cm^{-1}, which overestimate by 2.8%, 5.8%, 2.4%, and 0.7%, respectively, our observed frequencies. These

are typical deviations for the B3LYP functional used in frequency calculations of main group light metal hydrides.[9,10] Similar MP2 frequency calculations give four strong modes at 1652.3, 1281.0, 1097.1, and 687.1 cm^{-1}, which are slightly higher than the B3LYP values, and comparable to values given in the previous report.[29]

Corresponding experiments were done with Mg and pure HD and diagnostic bands for the identification of H−Mg(μ-H)$_2$Mg−H are observed. Three isotopomers are possible for the doubly D-substituted molecule, H−Mg(μ-HD)Mg−D, H−Mg-(μ-D)$_2$Mg−H, and D−Mg(μ-H)$_2$Mg−D, using the HD reagent, and very complicated spectra are thus expected. However, some isotopomers may be disfavored because of higher zero-point energies (ZPE). In the Mg−H stretching region new 1594.0 and 1592.6 cm^{-1} absorptions were observed in Mg + HD spectra and in the bending region 586.3 and 505.3 cm^{-1} bands appeared with the upper bands. A set of bands at 1169, 1145.0, 860.8, 811.0, 807.9, and 771.1 cm^{-1} track bands mentioned above and must be due to a common molecular species. In this case theoretical calculations are extremely helpful to make specific assignments. First, H−Mg(μ-D)$_2$Mg−H is the most favorable molecule at low temperature because of the lowest ZPE of all three isotopomers while D−Mg(μ-H)$_2$Mg−D is the highest. Second, the calculated frequencies for the Mg(μ-D)$_2$Mg subunit in H−Mg(μ-D)$_2$Mg−H are very close to this subunit in D−Mg-(μ-D)$_2$Mg−D and likewise H−Mg(μ-H)$_2$Mg−H is a good model for the Mg(μ-H)$_2$Mg subunit in D−Mg(μ-H)$_2$Mg−D. Two new bands observed at 860.8 and 771.1 cm^{-1} match the frequencies for the Mg(μ-D)$_2$Mg subunit. In addition the 1592.6 cm^{-1} band is appropriate for the Mg−H mode and the 505.3 cm^{-1} band for the bending mode. Hence, these bands are assigned to H−Mg(μ-D)$_2$Mg−H. B3LYP calculation gave IR active bands at 1632.1, 893.5, 788.5, and 509.6 cm^{-1}, which reproduced experimental values very well. Third, the calculated vibrational modes for the Mg(μ-HD)Mg subunit (B3LYP) in H−Mg(μ-HD)Mg−D are split to 1219.2 and 1180.8 cm^{-1} in the upper hydrogen region, and to 835.1 and 830.5 cm^{-1} in the lower deuterium region, which match the observed 1169, 1146.3, and 811.0, 807.9 cm^{-1} absorptions. In addition new 1594.0 and 1145.0 cm^{-1} bands are due to the Mg−H and Mg−D stretching modes and the 586.3 cm^{-1} band is due to the bending mode for this molecule, which are computed at 1636.6, 1180.7, and 588.4 cm^{-1}, respectively. Fourth, weak absorptions were observed for the higher energy D−Mg(μ-H)$_2$Mg−D isotopomer at 1204.9 and 655.5 cm^{-1}. Hence we conclude the $Mg_2H_2D_2$ isotopic identifications and the H−Mg(μ-H)$_2$Mg−H assignment.

In the experiment with H_2 + D_2 (50−50) MgH_2 and MgD_2 were produced in an approximately 2/1 ratio based on calculated isotopic intensities. Hence, their dimerization could produce Mg_2H_4 as well as $Mg_2H_2D_2$ in favorable yield. The 1587.1 and 1169.8 cm^{-1} bands in this experiment are due to H−Mg(μ-H)$_2$Mg−H and the 860.5 cm^{-1} band must be due to D−Mg-(μ-D)$_2$Mg−D. The strongest band (835 cm^{-1}) for H−Mg(μ-HD)MgD is not observed yet this isotopomer is the only mixed dimer of MgH_2 and MgD_2, so other mechanisms must be considered.

The absorptions of H−Mg(μ-H)$_2$Mg−H were also found in solid neon. Laser ablated Mg atom reaction with H_2 in excess neon generates MgH_2 monomer. With 240 nm photolysis the yield of MgH_2 increased 10-fold, and meanwhile new bands were produced at 1583.7, 1169.9, 1058.9, and 665.9 cm^{-1}. These bands are appropriate for the H−Mg(μ-H)$_2$Mg−H molecule based on comparison with observations in solid hydrogen. With D_2 in solid neon these bands shift to 1173.8, 860.8, 773.6, and 486.5 cm^{-1}. Experiments with Mg reaction HD in solid neon gave absorptions of H−Mg(μ-D)$_2$Mg−H at 862.1, 773.6, and 506.2 cm^{-1}, and for H−Mg(μ-HD)Mg−D at 1168.3, 812.5, and 589.7 cm^{-1}. Some weak bands for this isotopomer were not observed because of band broadness in solid neon.

The absorptions of H−Mg(μ-H)$_2$Mg−H in solid argon were tentatively assigned in our early work,[7] and the strongest of these at 1164.2 cm^{-1} is confirmed by comparison with our neon matrix absorptions. However, the solid argon matrix is more rigid and polarizable, and the dimerization of MgH_2 is strongly inhibited. As a result the yield of H−Mg(μ-H)$_2$Mg−H is very small. A similar case was found for the Al atom reaction with H_2: we trapped H_2−Al(μ-H)$_2$Al−H_2 in large yield in solid hydrogen and neon, but only very weak absorptions were observed in solid argon.[10]

The Mg_2H_4 molecule could in principle be formed from dimerization of either MgH_2 or Mg_2H_2 adding H_2 to give Mg_2H_4. Spontaneous formation of Mg_2H_4 is observed on annealing suggesting that no significant activation energy is required for exothermic reaction 3. This is in agreement with the spontaneous formation of solid MgH_2 on evaporation of the solid H_2 matrix.

$$2MgH_2 \rightarrow Mg_2H_4 \qquad (\Delta E = -27 \text{ kcal/mol (B3LYP)}) \quad (3)$$

$$Mg_2H_2 + H_2 \rightarrow Mg_2H_4 \qquad (\Delta E = -20 \text{ kcal/mol (B3LYP)}) \quad (4)$$

$$Mg_2 + 2H_2 \xrightarrow{UV} Mg_2H_4 \quad (5)$$

Some of the MgH_2 molecules from reaction 1 with high vibrational energy before relaxation can surmount the energy barrier to dimerize (reaction 3). The Mg_2H_2 molecules trapped in solid hydrogen after deposition could react with H_2 to give Mg_2H_4 through $\lambda > 320$ nm photolysis; however, $\lambda > 290$ nm and 240−380 nm irradiation gives far more Mg_2H_4 after Mg_2H_2 is gone.

Laser-ablated and excited Mg that does not react must relax to the ground ^1S_o state, which will not react with H_2, but will dimerize to Mg_2 as observed previously. This Mg_2 species absorbs strongly at 370 nm,[31] and Mg_2* reacts in the hydrogen matrix cage to give Mg_2H_4, reaction 5.

Mg_3H_6 and Mg_4H_8. In solid neon new bands at 1564.5 and 1551.6 cm^{-1} appeared on 240 nm photolysis and increased on further annealing to 10−12 K. With D_2 in solid neon the two bands shift to 1154.2 and 1140.6 cm^{-1} and with HD in neon at 1558.2 and 1544.9 cm^{-1} (Mg−H stretching), and 1132.7 and 1123.6 cm^{-1} (Mg−D stretching). Similar broad bands were also observed in solid H_2, D_2, and HD. The photolysis and annealing behaviors of these bands led us to consider higher polymer assignment.

DFT calculations were performed for Mg_3H_6 and Mg_4H_8, and single-bridged (cyclic)-Mg(H)-H− and double-bridged (chain) −Mg-(μ-H)$_2$− molecules converged (Figure 8). Although these two conformers have very close energies, the strongest IR active modes are very disparate based on single or double bridged metal−hydrogen−metal bonds. The single-bridged conformers show a much shorter bridged Mg−H bond than double bridged and as a result the vibration stretching mode of bridged Mg−H strongly couples with end Mg−H stretching motion. It is not surprising that the frequency for this mode is very close to Mg−H stretching in free MgH_2. However, for double-bridged conformers the bridged Mg−H bond is very close to the MgH_2 dimer HMg−(μ-H)$_2$−MgH and the strongest IR active modes are in the same region as observed for the MgH_2 dimer. As

shown in Table 3 very strong absorptions at 1599.9 cm^{-1} for s-Mg_3H_6 and at 1730.8 and 1618.1 cm^{-1} for s-Mg_4H_8 (s denotes single bridge) are calculated with the B3LYP functional, which basically agree with the observed 1564.5 and 1551.6 cm^{-1} bands. Several weak absorptions below these two bands appeared on annealing to higher temperature, which must be due to higher polymers with single bridged bond linkage. However, the calculated strong absorptions at 1204.5 cm^{-1} for d-Mg_3H_6 and 1178.5 cm^{-1} for d-Mg_4H_8 (d denotes double bridge) are not observed. It is very interesting to note in contrast that double bridged beryllium hydride polymer has been identified in solid hydrogen, which will be discussed in an upcoming paper.

The polymerization of MgH_2 is exothermic based on our initial calculations and this is the reason the bulk MgH_2 is very stable and the decomposition temperature is very high (360 °C).[2] As we observed in both solid hydrogen and neon s-Mg_3H_6 is trapped instead of d-Mg_3H_6 although the later is more exothermic. Higher polymers are obtained in the same way. It appears from the spectrum of the solid that higher 3-dimensional polymers revert to the double-bridged model.

$$Mg_2H_4 + MgH_2 \rightarrow \text{s-}Mg_3H_6 \qquad (\Delta E = -26 \text{ kcal/mol}) \quad (6)$$

$$Mg_2H_4 + MgH_2 \rightarrow \text{d-}Mg_3H_6 \qquad (\Delta E = -29 \text{ kcal/mol}) \quad (7)$$

$$\text{s-}Mg_3H_6 + MgH_2 \rightarrow \text{s-}Mg_4H_8 \qquad (\Delta E = -20 \text{ kcal/mol}) \quad (8)$$

MgH_2 Solid. Warming the previously described hydrogen samples to 10 K allowed the hydrogen host to evaporate, the $MgH_2(H_2)_n$ complexes to decompose, and a solid magnesium hydride film to form on the CsI substrate. This film exhibited broad 1160 and 560 cm^{-1} absorptions (Figure 3) and remained on the support at room temperature. The deuterium counterpart exhibited a broad 880 cm^{-1} absorption (H/D ratio 1.32).

The vibrational spectrum of solid magnesium hydride determined from neutron scattering contains broad bands at 72, 124, and 148 meV (580, 1000, and 1200 cm^{-1}).[5] Our solid MgH_2 film spectrum (Figure 3) reveals a broad 1000−1300 cm^{-1} flat-top band centered at 1160 cm^{-1} and a 560 cm^{-1} peak, which are in excellent agreement with the vibrational density of states from neutron scattering.[5] It appears that we have formed a solid MgH_2 film by allowing MgH_2 molecules to aggregate that is similar to that formed on Mg reacting with H_2 gas at 500 °C.

The 1000 and 1200 cm^{-1} vibrations in solid MgH_2 are probably due to bridge Mg−H−Mg bond stretching modes with neon matrix counterparts near 1059 and 1170 cm^{-1} for the H−Mg(μ-H)$_2$Mg−H molecule discussed above. The 1.95 Å solid X-ray Mg−H bond length[4] is slightly longer than our B3LYP value (1.875 Å) for bridge bonds in the latter molecule. We note that calculated lattice energy using a Born−Mayer model is −2906 kJ/mol as compared to the experimental Born−Haber cycle value of −2721 kJ/mol. This difference has been attributed to an appreciable covalent contribution to the bonding.[32]

MgH and Mg_2H. A strong band at 1427.1 cm^{-1} with satellites at 1429.5, 1430.6, and 1431.9 cm^{-1} appeared on deposition and reaction of Mg with H_2 in solid normal hydrogen. This band decreased on 240−380 nm photolysis (Figure 1c), but was restored in part on 193 nm irradiation (another experiment). In solid normal deuterium the counterparts were observed at 1042.8, 1044.4, 1045.9, and 1047.5 cm^{-1}. In solid HD two sets of bands at 1428.1, 1430.6, 1431.9, and 1433.5 cm^{-1} (Mg−H stretching region) and at 1042.6, 1044.3, 1045.5, and 1046.9 cm^{-1} (Mg−D stretching region) were obtained. This is appropriate for the diatomic MgH molecule. We note that the absorptions of Mg−H and Mg−D stretching modes in solid H_2, D_2, and HD are slightly shifted because of different interactions between trapped MgH (MgD) and surrounding H_2, D_2, or HD. In solid parahydrogen the site absorption of MgH was simplified: only a very sharp band at 1427.4 cm^{-1} and a weak site at 1429.9 cm^{-1} were observed.

In solid neon MgH and MgD give weak bands at 1431.3 and 1045.5 cm^{-1} and the assignment was confirmed by production of the same bands from the Mg atom reaction with HD in solid neon. The absorptions for MgH and MgD in neon are very close to gas-phase fundamentals at 1431.98 and 1045.85 cm^{-1}.[30]

In solid normal hydrogen a weak band at 1464.6 cm^{-1} appeared on deposition, decreased on $\lambda > 320$ nm photolysis, and was partly restored on 193 nm eximer irradiation (recall MgH was also partly restored on 193 nm photolysis). This band was favored by higher laser energy and located 37.5 cm^{-1} higher than the MgH stretching motion. In solid parahydrogen a similar band appeared at 1466.7 cm^{-1}. The deuterium counterpart was found at 1066.7 cm^{-1} for normal D_2 and 1068.7 cm^{-1} for ortho-D_2. With Mg in solid HD two bands at 1464.3 and 1067.8 cm^{-1} are associated with the bands observed in solid H_2 and D_2 (the solid molecular hydrogen matrix environments are different). In solid neon the counterpart bands were observed at 1470.0 cm^{-1} in the Mg−H region, 1070.9 cm^{-1} in the Mg−D region, and 1470.0 and 1070.9 cm^{-1} with HD. This is the only feature increased by 193 nm radiation in solid neon. Apparently only one H atom is involved in this vibration motion. The Mg_2H molecule is appropriate for this band.

Two isomers of Mg_2H, namely MgMgH amd MgHMg, were calculated with the B3LYP functional and MgMgH is energetically favored (Table 3). The predicted Mg−H stretching frequency at 1506.7 cm^{-1} matches our experimental observation very well. However, no band was observed for MgHMg.

The MgH is generated through energetic laser-ablated Mg atom reaction with H_2, which is endothermic by 72 kcal/mol for the ground Mg (3s, $^1S_0$) reaction with H_2 based on our B3LYP functional calculation or 74 kcal/mol from experiment.[33] However, excited Mg (3s3p, $^1P_1$) is sufficient to overcome this and activate the H−H bond efficiently to give MgH_2* and then decompose to MgH and H. Reaction 9 has been studied with pump−probe laser and far-wing laser scattering.[34−36]

$$Mg\ (3s3p) + H_2 \rightarrow MgH_2^* \rightarrow MgH + H \quad (9)$$

Mg_2H is probably formed by clustering with MgH, reaction 10, or by dissociation of HMgMgH, reaction 11.

$$Mg + MgH \rightarrow MgMgH \quad (10)$$

$$HMgMgH \xrightarrow{193\text{ nm}} H + MgMgH \quad (11)$$

Mg_2H_2. The sharp, weak absorption at 1486.1 cm^{-1} in solid n-H_2 decreased on irradiation like the 1064.8 cm^{-1} Mg_2H band. This band shifted to 1083.0 cm^{-1} with n-D_2, but unlike Mg_2H, different 1495.7 and 1088.9 cm^{-1} counterparts were observed with pure HD.

The counterpart absorption at 1496.4 cm^{-1} for the Mg atom reaction with H_2 in solid neon was produced on $\lambda > 240$ nm photolysis but decreased by 193 nm irradiation. With D_2 in neon this band shifted to 1088.9 cm^{-1}, but for HD in neon two corresponding bands at 1508.9 and 1099.3 cm^{-1} were observed. These shifts characterize two coupled Mg−H stretching modes, which interact slightly more than in MgH_2. Calculations with

TABLE 5: Comparison of Matrix Frequencies (cm^{-1}) for MgH, MgH_2, and Mg_2H_4

molecule	gas[a]	Ne	p-H_2[b]	n-H_2[c]	Ar[d]	Kr[e]	Xe[e]
MgH	1431.98	1431.3	1427.4	1427.1	1422.1		
MgD	1045.85	1045.5	1043.0	1042.8	1037.7		
H/D	1.3692	1.3690	1.3686	1.3685	1.3690		
MgH_2	1588.67	1576.8	1577.4	1569.5	1571.9	1558	1544
MgD_2		1163.2	1163.9	1161.4	1157.1	1153	1144
H/D		1.3556	1.3555	1.3514	1.3546	1.351	1.350
Mg_2H_4		1169.9	1168.2	1170.5	1164.2		
		1058.9	1057.1	1058.7			

[a] References 6 and 30. [b] 99% p-H_2, but for MgD and MgD_2 this is 98% o-D_2. [c] For MgD and MgD_2 this is n-D_2. [d] Reference 7. [e] Reference 8.

the B3LYP functional give a linear HMgMgH geometry with the Mg−H stretching mode at 1551.3 cm^{-1} and Mg−D at 1119.2 cm^{-1}. In addition HMgMgD stretching modes were predicted at 1561.8 and 1127.0 cm^{-1}, 9.5 cm^{-1} above the all-H mode and 7.8 cm^{-1} above the all-D mode (experimental shifts are 12.5 and 9.4 cm^{-1} in solid neon, and 9.6 and 5.9 cm^{-1} in solid hydrogen). This means that an unobserved high-symmetry mode is higher in frequency (i.e., the σ_u mode for the linear molecule, Table 3). Such excellent agreement confirms the observation and characterization of linear HMgMgH. The bands assigned formerly[7] to cyclic $(MgH)_2$ are probably due to $H(MgH)_2H$ or other higher magnesium hydride. Thus, the higher energy cyclic $(MgH)_2$ species remains unobserved.

Mg_2H_2 is produced from either the Mg_2 reaction with H_2 or the dimerization of MgH. Solid neon experiments gave a clue that Mg_2 is exited by $\lambda > 240$ nm photolysis and combined with H_2 to give Mg_2H_2 (reaction 12) while MgH is not changed. The bonding of Mg_2H_2 is basically the same as that of the magnesium cluster Grignard reagent, where the strong Mg−Mg bond stabilizes this reactive species. In solid hydrogen larger magnesium clusters (HMg_xH) are probably formed.

$$Mg_2 + H_2 \xrightarrow{UV} Mg_2H_2 \quad (12)$$

$$2MgH \rightarrow Mg_2H_2 \quad (13)$$

Mg_2H_3. In solid normal hydrogen two bands at 1105.9 and 985.5 cm^{-1} appeared on deposition, decreased on 380 and 240 nm photolysis, and were restored partly on annealing. The deuterium counterparts were found at 813.1 and 718.5 cm^{-1} in solid normal D_2. Two modes are just below the double bridged $-Mg(\mu\text{-}H)_2Mg-$ vibrations in Mg_2H_4 and a similar structure for the new molecule is suggested. Recall two stretching frequencies of double bridged $Al(\mu\text{-}H)_2Al$ in Al_2H_5 radical are a few wavernumbers below the same modes for dialane,[11] and we believe the Mg_2H_3 radical with a double-bridged $Mg(\mu\text{-}H)_2Mg$ bond is the case here. First the chemical behavior of this species is very active, and it grows at the expense of both MgH and MgH_2 on early annealing in our experiments. Second B3LYP calculation gave two conformers, single-bridged (HMg(H)MgH), s-Mg_2H_3, and double-bridged ($HMg(\mu\text{-}H)_2Mg$), d-Mg_2H_3, and the latter is 12.1 kcal/mol lower in energy. The stronger and a weaker double-bridged modes of d-Mg_2H_3 were predicated at 1162.2 and 1042.8 cm^{-1}, which match observed values very well after the same adjustment as for Mg_2H_4. Finally, the HD spectra gave additional information for this radical: a stronger band at 1013.9 cm^{-1} and a weaker band at 814.6 cm^{-1} in solid HD formed on deposition and disappeared on 240 nm photolysis. Four possible isotopomers with HD, $HMg(\mu\text{-}HD)_2Mg$, $DMg(\mu\text{-}HD)_2Mg$, $HMg(\mu\text{-}D)_2Mg$, and $DMg(\mu\text{-}H)_2Mg$, are computed, and for each of these the strongest absorptions are found at 1105.6, 1103.8, 836.7, and 1162.0 cm^{-1}, respectively. Obviously, the 1013.9 cm^{-1} band is due to $HMg(\mu\text{-}HD)_2Mg$ and $DMg(\mu\text{-}HD)_2Mg$ and the 814.6 cm^{-1} band is due to $HMg(\mu\text{-}D)_2Mg$ based on calculated frequencies with scaled corrections. Again the preference is for the heavier isotope in the bridge position. The combination of MgH_2 and MgH is exothermic by 25.6 kcal/mol (B3LYP).

$$MgH + MgH_2 \rightarrow d\text{-}Mg_2H_3 \quad (14)$$

Matrix Shifts. The large number of new magnesium hydride species provides further subjects for unusual matrix shifts. First, MgH behaves quite normally in that the fundamental frequency decreases from left to right in Table 5. Note that the MgH frequency in p-H_2 is red-shifted 4.6 cm^{-1} from the gas phase whereas the frequency is red-shifted 4.9 cm^{-1} in n-H_2. Analogous results are found for MgD in o-D_2 and n-D_2. The H/D frequency ratios are 1.3692−1.3690 for gas, Ne, and Ar frequencies, but slightly lower 1.3686 and 1.3685 values are observed in the solid hydrogens. This is consistent with slightly less H motion in the Mg−H vibration due to greater interaction with the hydride and the hydrogen matrix cage.

The MgH_2 frequencies reveal a small difference from the trend found for MgH in different matrices: The p-H_2 frequency for MgH_2 is 0.6 cm^{-1} higher than the neon value, and the o-D_2 frequency for MgD_2 is 0.7 cm^{-1} higher than the neon value. The n-H_2 and n-D_2 frequencies are lower than the neon values and the gas-phase values,[6] as expected. The p-H_2 environment perturbs the linear MgH_2 molecule less than neon even though very weak complexes are formed with H_2. The H/D ratios again provide evidence for less H motion in n-H_2, Kr, and Xe due to stronger interaction with the hydride. Figure 4 compares the spectra in normal and $J = 0$ enriched molecular hydrogens.

Note that the matrix shifts for MgH_2 are larger than those for MgH even with p-H_2. This is due to stronger H_2 complex formation with MgH_2 than with MgH: even though bond polarity is the same (B3LYP Mulliken charges are −0.19 on H in both MgH and MgH_2), the Mg charge is +0.38 in MgH_2 as compared to +0.19 in MgH.

Finally, $HMg(\mu\text{-}H)_2MgH$ is unusual in that the n-H_2 frequencies are highest. However, these are Mg−H−Mg bridge bond stretching modes, and a stronger interaction may help relieve electron deficiency and strengthen the bridge bonds. The same relationship was found for dialane, $H_2Al(\mu\text{-}H)_2AlH_2$. The terminal Al−H modes are slightly higher in p-H_2, but the bridge Al−H−Al modes are slightly lower in p-H_2 as compared to n-H_2.[11]

Conclusions

Laser ablated Mg atoms react with H_2 in excess neon and hydrogen on co-deposition to give MgH and MgH_2. The absorption of MgH at 1431.3 cm^{-1} in solid neon is essentially the same as detected in the gas phase at 1431.98 cm^{-1}. In solid parahydrogen MgH shifts to 1427.4 cm^{-1} showing weak interaction with surrounding H_2. The Mg−H stretching mode

of MgH_2 at 1576.2 cm^{-1} in solid neon is 12.5 cm^{-1} lower than the recent gas-phase value,[6] indicating that the HMgH molecule interacts with surrounding neon atoms stronger than MgH. In fact stronger interaction was found for HMgH with H_2 in solid H_2 based on two strong H−H stretching modes induced by MgH_2. We suggest H_2 molecules are associated side-on to Mg and end-on to H surrounding HMgH, and theoretical calculations support this model.

Dimagnesium hydrides, Mg_2H, Mg_2H_2, Mg_2H_3, and Mg_2H_4, were identified using isotopic substitutions and theoretical calculations. A strong Mg−Mg bond is favored in hydrogen-deficient molecules such as Mg_2H and Mg_2H_2, while double bridged Mg−H−Mg bonds were found in Mg_2H_3 and Mg_2H_4. The latter molecule $HMg(\mu\text{-}H)_2MgH$ is analogous to dialane[9−11] $H_2Al(\mu\text{-}H)_2AlH_2$, but both terminal and bridged bonds are computed to be 7.8% longer in the magnesium compound.

Acknowledgment. We gratefully acknowledge support from N.S.F. Grant CHE 00-78836 and 03-52487.

References and Notes

(1) (a) Schlapbach, L.; Zuttel, A. *Nature* **2001**, *414*, 353. (b) Dresselhaus, M. S.; Thomas, I. L. *Nature* **2001**, *414*, 332.
(2) Aldridge, S.; Downs, A. J. *Chem. Rev.* **2001**, *101*, 3305.
(3) Grochala, W.; Edwards, P. P. *Chem. Rev.* **2004**, *104*, 1283.
(4) Zachariasen, W. H.; Holley, C. E.; Stampfer, J. F. *Acta Crystallogr.* **1963**, *16*, 352.
(5) Santisteban, J. R.; Cuello, G. J.; Dawidowski, J.; Fainstein, A.; Peretti, H. A.; Ivanov, A.; Bermejo, F. J. *Phys. Rev. B* **2000**, *62*, 37.
(6) (a) Shayesteh, A.; Appadoo, D. R. T.; Gordon, I.; Bernath, P. F. *J. Chem. Phys.* **2003**, *119*, 7785. (b) Shayesteh, A.; Appadoo, D. R. T.; Gordon, I.; Bernath, P. F. *Can. J. Phys.* **2004**, *82*, 947.
(7) Tague, T. J., Jr.; Andrews, L. *J. Phys. Chem.* **1994**, *98*, 8611.
(8) McCaffrey, J. G.; Parnis, J. M.; Ozin, G. A.; Breckenridge, W. H. *J. Phys. Chem.* **1985**, *89*, 4945.
(9) Andrews, L.; Wang, X. *Science* **2003**, *299*, 2049.
(10) Wang, X.; Andrews, L.; Tam, S.; DeRose, M. E.; Fajardo, M. *J. Am. Chem. Soc.* **2003**, *125*, 9218.
(11) Andrews, L.; Wang, X. *J. Phys. Chem. A* **2004**, *108*, 4202 (Al + H_2).
(12) Wang, X.; Andrews, L. *J. Phys. Chem. A* **2003**, *107*, 11371 (Ga + H_2).
(13) Andrews, L.; Wang, X. *Angew. Chem., Int. Ed.* **2004**, *43*, 1706.
(14) Wang, X.; Andrews, L. *J. Phys. Chem. A* **2004**, *108*, 4440 (In + H_2).
(15) Wang, X.; Andrews, L. *J. Phys. Chem. A* **2004**, *108*, 3396 (Tl + H_2).
(16) Andrews, L.; Citra, A. *Chem. Rev.* **2002**, *102*, 885 and references therein.
(17) Andrews, L. *Chem.* Soc. *Rev.* **2004**, *33*, 123 and references therein.
(18) Wang, X.; Andrews, L. *J. Phys. Chem. A* **2004**, *108*, 1103 ($(H_2)_n(H^-)$).
(19) Andrews, L.; Wang, X. *Rev. Sci. Instrum.* **2004**, *75*, 3039.
(20) Wang, X.; Wolfe, B.; Andrews, L. *J. Phys. Chem. A* **2004**, *108*, 5169.
(21) Frisch, M. J.; Trucks, G. W.; Schlegel, H. B.; Scuseria, G. E.; Robb, M. A.; Cheeseman, J. R.; Zakrzewski, V. G.; Montgomery, J. A., Jr.; Stratmann, R. E.; Burant, J. C.; Dapprich, S.; Millam, J. M.; Daniels, A. D.; Kudin, K. N.; Strain, M. C.; Farkas, O.; Tomasi, J.; Barone, V.; Cossi, M.; Cammi, R.; Mennucci, B.; Pomelli, C.; Adamo, C.; Clifford, S.; Ochterski, J.; Petersson, G. A.; Ayala, P. Y.; Cui, Q.; Morokuma, K.; Malick, D. K.; Rabuck, A. D.; Raghavachari, K.; Foresman, J. B.; Cioslowski, J.; Ortiz, J. V.; Stefanov, B. B.; Liu, G.; Liashenko, A.; Piskorz, P.; Komaromi, I.; Gomperts, R.; Martin, R. L.; Fox, D. J.; Keith, T.; Al-Laham, M. A.; Peng, C. Y.; Nanayakkara, A.; Gonzalez, C.; Challacombe, M.; Gill, P. M. W.; Johnson, B.; Chen, W.; Wong, M. W.; Andres, J. L.; Gonzalez, C.; Head-Gordon, M.; Replogle, E. S.; Pople, J. A. *Gaussian 98*, Revision A.11.4, Gaussian, Inc.: Pittsburgh, PA, 1998, and references therein.
(22) Gush, H. P.; Hare, W. F.; Allin, E. J.; Welsh, H. L. *Can. J. Phys.* **1960**, *38*, 176.
(23) Crane, A.; Gush, H. P. *Can. J. Phys.* **1966**, *44*, 373.
(24) Andrews, L.; Wang, X. *J. Phys. Chem. A* **2004**, *108*, 3879.
(25) Momose, T.; Shida, T. *Bull. Chem. Soc. Jpn.* **1998**, *71*, 1.
(26) Pople, J. A.; Luke, B. T.; Frisch, M. J.; Binkley, J. S. *J. Phys. Chem.* **1985**, *89*, 2198.
(27) Tschumper, G. S.; Schaefer, H. F., III *J. Chem. Phys.* **1998**, *108*, 7511.
(28) Von Szentpaly, L. *J. Phys. Chem. A* **2002**, *106*, 11945.
(29) Kaupp, M.; Schleyer, P. v. R. *J. Am. Chem. Soc.* **1993**, *115*, 11202.
(30) Lemoine, B.; Demuynck, C.; Destombes, J. L.; Davies, P. B. *J. Chem. Phys.* **1988**, *89*, 673.
(31) Miller, J. C.; Andrews, L. *J. Am. Chem. Soc.* **1978**, *100*, 2966.
(32) Stander, C. M.; Pacey, R. A. *J. Phys. Chem. Solids* **1978**, *39*, 829.
(33) Huber, K. P.; Herzberg, G. *Spectra of Diatomic Molecules*; Van Nostrand Reinhold: New York, 1979.
(34) (a) Kleiber, P. D.; Lyyra, A. M.; Sando, K. M.; Heneghan, S. P.; Stwalley, W. C. *Phys. Rev. Lett.* **1985**, *54*, 2003. (b) Kleiber, P. D.; Lyyra, A. M.; Sando, K. M.; Zafiropulos, V.; Stwalley, W. C. *J. Chem. Phys.* **1986**, *85*, 5493.
(35) (a) Breckenridge, W. H.; Wang, J. H. *Chem. Phys. Lett.* **1987**, *137*, 195. (b) Breckenridge, W. H. *J. Phys. Chem.* **1996**, *100*, 14840.
(36) Liu, D. K.; Lin, K. C. *Chem. Phys. Lett.* **1997**, *274*, 37.